Paleoceanography and Paleoclimatology

Supporting Information for

Calcium carbonate dissolution triggered by high productivity during the last glacial-interglacial interval at the deep western South Atlantic

J.Y. SUAREZ-IBARRA[1,2], C.F. FROZZA[1], S.M. PETRÓ[3], P.L. PALHANO[1], M.A.G. PIVEL[4]

[1]Programa de Pós-Graduacão em Geociências, Instituto de Geociências, Universidade Federal do Rio Grande do Sul, Av. Bento Gonçalves, 9500, Cx. P. 15001, 91501-970, Porto Alegre, RS, Brazil.
[2]Ústav Geologie a Paleontologie, Přírodovědecká fakulta, Univerzita Karlova, Albertov 6, Praha 2, 12843, Czech Republic, present address.
[3]ITT FOSSIL - Instituto Tecnológico de Micropaleontologia, Universidade do Vale do Rio dos Sinos, Av. UNISINOS, 950, 93022-750, São Leopoldo, RS, Brazil.
[4]Instituto de Geociências, Universidade Federal do Rio Grande do Sul, Av. Bento Gonçalves, 9500, Cx. P. 15001, 91501-970, Porto Alegre, RS, Brazil.

Contents of this file

Introduction

The present Supporting Information file presents data for: i) other analyzed cores (Table S1), ii) the Sea Surface Temperature (SST) residuals (Figure S1), iii) the age model construction (Figure S1, Table S2 and Table S3), as well as iv) the appendix of planktonic Foraminifera species (Appendix S1).

Table S1

In the manuscript Figure 1 are shown the core SAT-048A location, as well as the location of the other analyzed cores. Names, coordinates, and depths below sea level of the mentioned cores are shown in Table S1.

Table S1. Location of the other analyzed cores, all recovered from the western South Atlantic.

Core	Lat	Long	Depth (mbsl)
SAN-76	24°25'S	42°16'W	1682
GL-852	25°0'S	43°33'W	1938
GeoB2107-3	27°10'S	46°27'W	1048
GeoB2104-3	27.3°S	46.4°W	1500
JPC-17	27°41'S	46°29'W	1627
SAT-048A	29°11'S	47°15'W	1542
SIS-188	29°22'S	47°28'W	1514

Figure S1

The SST estimates at 100 m waters below sea level, performed on the present study, are show in manuscript Figure 4. Residual of this reconstruction is showed in Figure S1. The 95% of the residuals are located between 2.5 and -2.5°C, while the 90% are between 1.8 and -1.8°C.

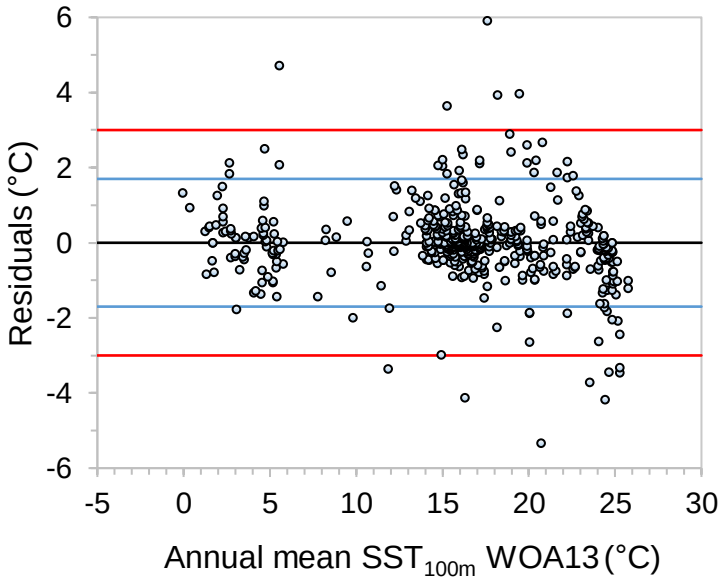

Figure S1. Residuals vs. Annual mean SST estimates at 100 m waters below sea level for core SAT048A. Red lines encompass 95% of the residuals (between 2.5 and -2.5°C) and blue lines encompass 90% (between 1.8 and -1.8°C).

Text S1.

From the 54 samples, a total of 21,962 specimens of planktonic Foraminifera were classified into 28 morphospecies (supplemental material). A total of 4878 specimens of benthic Foraminifera were counted. Table S1 lists the morphospecies, total relative abundance and total absolute abundance in descending order. The dominant species in the associations were *Globigerinoides ruber albus*, with a maximum relative abundance of 25.32%, followed by *Globigerinita glutinata* (15.56%) and *Globigerina bulloides* (15.56%). Other representative but less abundant species are *Neogloboquadrina incompta* (8.57%), *Globigerinoides ruber ruber* (8.22%) and *Globoconella inflata* (7.69%).

Other species, with total relative abundances between 5 and 1% are (in decreasing order): *Trilobatus trilobus*, *Globoturborotalita tenellus, Neogloboquadrina dutertrei, Globorotalia scitula, Globoturborotalita rubescens, Globigerinella calida, Globorotalia truncatulinoides* (R)*, Globorotalia crassaformis* and *Globorotalia truncatulinoides* (L).

Finally, species with extremely low total absolute abundance (> 1%) are *Candeina nitida, Globigerina falconensis, Globigerinella siphonifera, Globigerinoides conglobatus, Globorotalia hirsuta, Globorotalia menardii*, *Globorotalia tumida, Neogloboquadrina pachyderma, Orbulina universa, Pulleniatina obliquiloculata, Trilobatus sacculifer, Turborotalita humilis* and *Turborotalita quinqueloba.*

Age Model

The performing results of the rBacon package for core SAT-048A are shown in Figure S2. It is possible to see the ^{14}C correlation points, as wells as the identified Laschamp geomagnetic excursion (Savian et al., submitted).

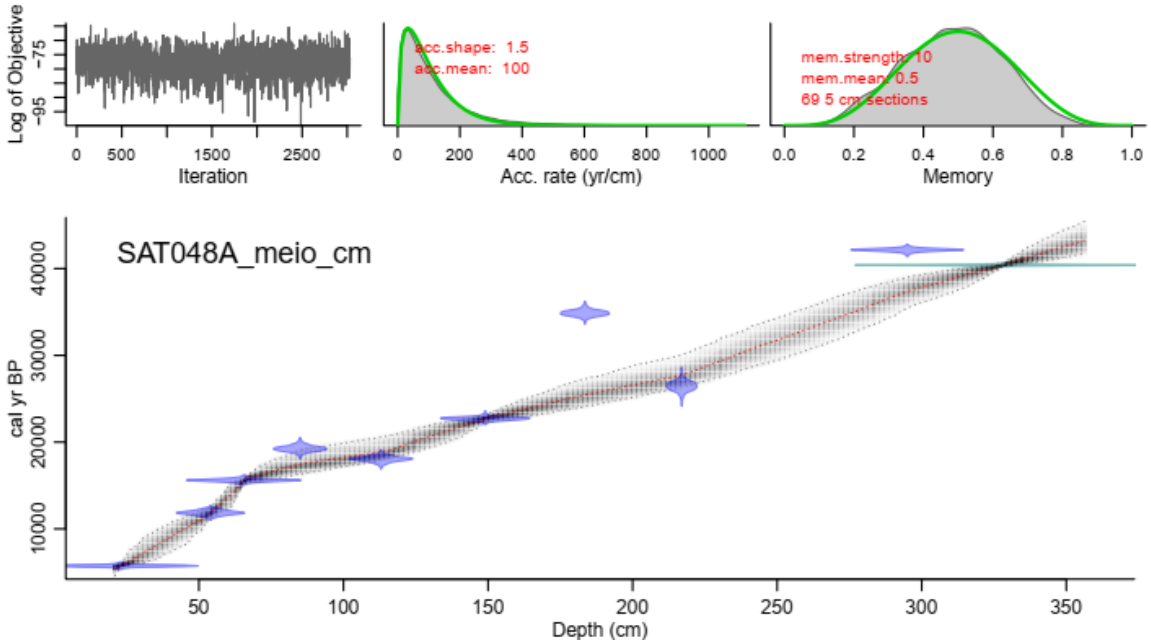

Figure S2. Age-depth plot for core SAT048A (bottom panel). The red stippled line indicates the mean age-depth model, 95% confidence ranges indicated by dark-grey stippled curves and calibrated dates in blue. Upper panels from left to right display (1) the Markov chain Monte Carlo (MCMC) iterations, the prior (green curves) and posterior (grey histograms) distributions for (2) the sedimentation rate and (3) memory.

The AMS ^{14}C results of core SAT-048A (Frozza et al., 2020) are shown in Table S2. The Marine Reservoir Correction Database (Delta R= -85 +/-40) is based on ages from Nadal de Masi (1999), Angulo et al. (2005), and Alves et al. (2015). Rbacon package (Blaauw & Christen, 2011; version 2.4.2), for open source R software (R Core Team, 2020), used the calibration curve Marine20 (Heaton et al., 2020).

Table S2. SAT-048A (Frozza et al., 2020) AMS ^{14}C ages.

Sample depth (cm)	LAC-UFF sample code	Species	Age ^{14}C (ka BP)	Error (ka)
23	170059	*G. menardii*	5.226	0.028
23	170209	*G. ruber*	5.471	0.032
54	180167	*G. ruber*	10.594	0.117
65	190321	*G. ruber*	13.548	0.038
85	180168	*G. ruber*	16.599	0.212
113	180169	*G. ruber*	15.531	0.185
149	190704	*G. ruber*	19.536	0.104
183.5	190323	*G. ruber*	31.174	0.271
217	180170	*G. ruber*	22.997	0.451
295	190540	*G. ruber*	38.997	0.260

Table S2 shows data the radiocarbon data published by Frozza et al., 2020 used for the former age model.

Table S3. SAT-048A data points for age model building on rbacon package.

LabID	Age	Error	Depth_cm	cc	delta.R	delta.STD
LACUFF170059	5226	28	23	2	-85	40
LACUFF170209	5471	32	23	2	-85	40
LACUFF180167	10594	117	54	2	-85	40
LACUFF190321	13548	38	65.5	2	-85	40
LACUFF180168	16599	212	85	2	-85	40
LACUFF180169	15531	185	113	2	-85	40
LACUFF190704	19536	104	149	2	-85	40
LACUFF190323	31174	271	183.5	2	-85	40
LACUFF180170	22997	451	217	2	-85	40
LACUFF190540	38997	260	295	2	-85	40
Laschamp	41000	0	328	0	0	0

Table S3 shows data used for the age model (Figure S2) building. Laschamp (Table S3) correlation point is from Savian et al. (submitted).

Appendix S1. List of the species/morphospecies/subspecies identified and their total relative and absolute abundances.

Species/ Morphospecies/subspecies	Total relative abundance (%)	Total absolute abundance
Globigerinoides ruber albus	25.32	5573
Globigerinita glutinata	15.56	3391
Globigerina bulloides	15.56	3355
Neogloboquadrina incompta	8.57	1892
Globigerinoides ruber ruber	8.22	1828
Globoconella inflata	7.69	1701
Trilobatus trilobus	2.22	492
Globoturborotalita tenellus	2.22	480
Neogloboquadrina dutertrei	1.64	371
Globorotalia scitula	1.50	322
Globoturborotalita rubescens	1.46	314
Globigerinella calida	1.29	292
Globorotalia truncatulinoides (R)	1.28	295
Globorotalia crassaformis	1.28	289
Globorotalia truncatulinoides (L)	1.16	258
Triolobatus sacculifer	0.93	212
Globigerina falconensis	0.89	193
Globorotalia hirsuta	0.62	135
Globigerinella siphonifera	0.41	93
Globorotalia menardii	0.37	77
Orbulina universa	0.36	79
Turborotalita quinqueloba	0.32	67
Globigerinoides conglobatus	0.32	70
Neogloboquadrina pachyderma	0.24	54
Pulleniatina obliquiloculata	0.21	44
Globorotalia tumida	0.07	16
Turborotalita humilis	0.04	9
Candeina nitida	0.04	8

References

Alves, E., Macario, K., Souza, R., Pimenta, A., Douka, K., Oliveira, F., Chanca, I., & Ângulo, E. (2015). Radiocarbon reservoir corrections on the Brazilian coast from pre-bomb marine shells. *Quaternary Geochronology*, 29, 30–35. doi:10.1016/j.quageo.2015.05.006

Angulo, R.J., de Souza, M.C., Reimer, P.J., & Sasaoka, S.K. (2005). Reservoir effect of the southern and southeastern Brazilian coast. *Radiocarbon*, 47, 67–73. doi:10.1017/S0033822200052206

Blaauw, M., & Christen, J.A. (2011). Flexible Paleoclimate Age-Depth Models using autoregressive gamma process. *Bayesian Analysis,* 6(3), 457–474. doi:10.1214/11-BA618

Frozza, C.F., Pivel, M.A.G., Suárez-Ibarra, J.Y., Ritter, M.N., &, Coimbra, J.C., 2020. Bioerosion on late Quaternary planktonic Foraminifera related to paleoproductivity in the western South Atlantic. *Paleoceanography and Paleoclimatology*, 35, e2020PA003865. doi:10.1029/2020PA003865

Heaton, T., Köhler, P., Butzin, M., Bard, E., Reimer, R., Austin, W., … Skinner, L. (2020). Marine20—The Marine Radiocarbon Age Calibration Curve (0–55,000 cal BP). *Radiocarbon* 62 (4), 779-820. doi:10.1017/RDC.2020.68

Lisiecki, L.E., & Stern, J.V. (2016). Regional and global benthic $\delta^{18}O$ stacks for the last glacial cycle. *Paleoceanography*, 31 (10), 1368–1394. doi:10.1002/2016PA003002

Nadal De Masi, M. A. (1999). *Prehistoric hunter-gatherer mobility on the southern Brazilian coast: Santa Catarina Island*. Ph.D. Thesis, Stanford University, Palo Alto, CA (unplublished).

R Core Team. (2020). *R: a language and environment for statistical computing*. Vienna, Austria: R Foundation for Statistical Computing. http://www.R-project.org/

Savian, J.F., Pivel, M.A.G., Frigo, E., Rocha, J.A., Lopes, C.T., Suárez-Ibarra, J.Y., Coimbra, J.C., Petró, S.M., Leonhardt, A., Callefo, F., Hartmann, G.A., Braga, A.H., Trindade, R.I.F., Rodelli, D., & Jovane, L. Environmental magnetic record of sediments from the western South Atlantic since Marine Isotope Stage 3. Paper submitted to *Global & Planetary Change*.